ANALYZING IMAGING BIOMARKERS FOR TRAUMATIC BRAIN INJURY USING 4D MODELING OF LONGITUDINAL MRI

Bo Wang[†,‡], *Marcel Prastawa*[†,‡], *Andrei Irimia*[§], *Micah C. Chambers*[§],

Neda Sadeghi[†], *Paul M. Vespa*[♮], *John D. van Horn*[§], *Guido Gerig*[†,‡*]

[†] Scientific Computing and Imaging Institute,
[‡] School of Computing,
University of Utah

[§] Laboratory of Neuro Imaging,
[♮] Brain Injury Research Center,
University of California at Los Angeles

ABSTRACT

Quantitative imaging biomarkers are important for assessment of impact, recovery and treatment efficacy in patients with traumatic brain injury (TBI). To our knowledge, the identification of such biomarkers characterizing disease progress and recovery has been insufficiently explored in TBI due to difficulties in registration of baseline and follow-up data and automatic segmentation of tissue and lesions from multimodal, longitudinal MR image data. We propose a new methodology for computing imaging biomarkers in TBI by extending a recently proposed spatiotemporal 4D modeling approach in order to compute quantitative features of tissue change. The proposed method computes surface-based and voxel-based measurements such as cortical thickness, volume changes, and geometric deformation. We analyze the potential for clinical use of these biomarkers by correlating them with TBI-specific patient scores at the level of the whole brain and of individual regions. Our preliminary results indicate that the proposed voxel-based biomarkers are correlated with clinical outcomes.

Index Terms— Imaging biomarkers, longitudinal MRI, correlation analysis, clinical outcome.

1. INTRODUCTION

A typical approach for identification of important imaging biomarkers is the correlation of image-derived features with clinical scores. Most previous work in this respect explores TBI outcome using biomarkers derived from diffusion tensor imaging (DTI) [1, 2, 3, 4] because certain injury types (such as diffuse axonal injury, DAI) are difficult to detect via structural computed tomography (CT) and magnetic resonance imaging (MRI). Studies on the use of structural or volumetric measures as biomarkers are limited due to the difficulties in segmenting and registering MR images presenting severe TBI [5]. Earlier research has been limited to single time

point analysis [1, 2], while recent contributions have implemented longitudinal analyses [3, 4] and, due to the difficulty of registering images between time points, previous longitudinal analyses have not typically gone beyond correlating imaging findings at the level of the whole brain to clinical score recorded at the same time point. To our knowledge, longitudinal analysis of local brain changes, obtained via spatiotemporal analysis of multimodal serial image data with TBI, has not been presented yet.

Spatiotemporal analysis in TBI imaging is challenging because large geometric, appearance and topology changes present difficulties for registration across time points and for tissue and lesion segmentation [6]. In particular, over the time course between impact and chronic stage, structures may deform and lesions can disappear or appear due to intervention, recovery or formation of new injuries. A recently developed method for spatiotemporal model construction [7] is capable of handling topological changes by using personalized atlas construction and estimation of regions undergoing alterations of topology. The method generates segmentation labels of tissue and lesion classes, probability of local topological changes, and temporal deformations. In this paper, we are building on this technology and propose new methods for computing surface- and voxel-based imaging biomarkers. These biomarkers include measures of cortical thickness, volumes of brain lobes and tissue deformations. The potential of our proposed methods to identifying imaging biomarkers of TBI temporal evolution is illustrated using five subjects with different types and severity of trauma.

2. METHOD

2.1. Spatiotemporal 4D modeling

Given multimodal images at time point t denoted by $I^t = \{I(x_1), \ldots, I(x_N)\}^t$ with N voxels indexed by positions x and M_t the number of channels, outputs of the spatiotemporal model construction [7] are a set of labels L^t at each time point t which contains k_t labels of all healthy and pathological classes and a diffeomorphic mapping h_t between each

time point t to the personalized atlas space. By composing h_t between time points, we obtain the deformation $T_{i,j}$ from time point i to j (see Fig. 1).
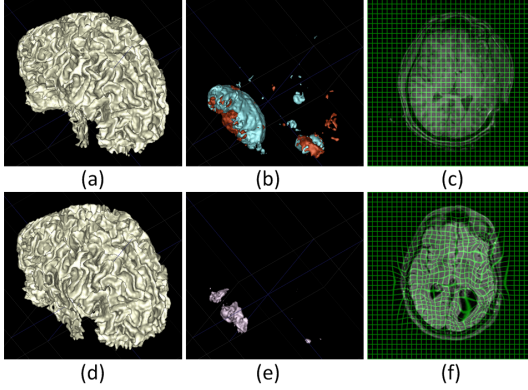
Fig. 1. Spatiotemporal model for a subject with severe TBI. Top: 3D display of WM (a), lesions (b) and (c) regular grid for the acute time point. Bottom: Same displays for chronic time point (d) and (e), and deformation mapping from actue to chronic shown in (f).

2.2. Surface-based imaging biomarkers

Algorithm 1 Compute cortical thickness and change

Input: Segmentation labels L^t at time points i, j, deformations h_i and h_j between time points i, j to the atlas space.
Output: Cortical thickness C_i and C_j on WM surface of time points i, j, and cortical thickness change C_{j-i} between time point i and j using $j - i$ on WM surface of time point i.
for $t =$ each time point of i, j **do**
  1: Extract WM surface $\rightarrow S_t$.
  2: Compute distance map to outer GM boundary $\rightarrow D_t$
  3: Evaluate the value of cortical thickness using D_t at each point on WM surface $S_t \rightarrow C_t$.
end for
4: Compose the the transforms h_i and h_j to get mapping from time point j to i: $T_{j,i} = h_j \circ h_i^{-1}$.
5: Compute cortical thickness change at each location
$$V_{j-i} = D_j \circ T_{j,i} - D_i.$$
6: Evaluate the value of cortical thickness change V_{j-i} at each point on WM surface S_i of time point $i \rightarrow C_{j-i}$.
7: Report C_i, C_j as cortical thickness at time i and j. Report C_{j-i} as the changes between time points i and j.

Given the spatiotemporal model with segmentation labels and deformations, we can compute surface-based features at each time point and between time points. In Algorithm 1, we show our method for computing cortical thickness at each time point and its changes between time points. We use distance transform for cortical thickness computation which is

made freely available as the ARCTIC package[1]. The primary reason for implementing this method was to avoid the generation of topologically correct brain surfaces as required in tools designed for high-quality normal appearing brain imaging, and thus its robustness to noise and changes induced by lesions. Algorithm 1 is generic and can be generalized to other surface-based measures such as displacement and curvature on the surface.

We analyze the surface-based measures through their sample means and histograms. The cortical thickness feature in particular is modeled as a beta distribution, motivated by the observation that the histograms are unimodal and non-symmetric. Longitudinal changes in these measures are computed through distances between sample means and distances between histograms, here using the symmetrized Kullback-Leibler divergence to measure distance between the beta distributions. Given $X_1 \sim \text{Beta}(\alpha, \beta)$ and $X_2 \sim \text{Beta}(\alpha', \beta')$, the distance between these surface based random variables is $D(X_1, X_2) = \frac{1}{2}(D_{\text{KL}}(X_1, X_2) + D_{\text{KL}}(X_2, X_1))$.

2.3. Voxel-based imaging biomarkers

We also explore voxelwise morphometric features as biomarkers, particularly volume and deformation measures. Volumetric measures are directly obtained from the spatiotemporal modeling via the 4D tissue segmentation, and deformation measures are obtained from the diffeomorphic deformations across time points, using the log of the Jacobian determinant as the deformation measure. Specifically, given the diffeomorphisms h_i and h_j between time points i, j to the atlas space, we obtain the mapping from i to j via composition, $T_{i,j} = h_i \circ h_j^{-1}$ and then compute log Jacobian determinant $\log |D \ T_{i,j}|$ where D is the differential operator. The influence of lesioned regions was reduced by masking.

2.4. Lobe-based analysis

So far in sections 2.2 and 2.3, biomarkers are defined over the whole brain. We investigate the relationship between the image findings in certain parts of the brain to clinical scores by subdividing the brain into major lobes. The methodology for parcellating the TBI brains into these lobes is presented in Algorithm 2 by using a healthy brain template. Fig. 2

---

[1]http://www.nitrc.org/projects/arctic/.
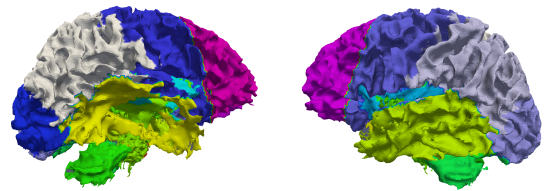
Fig. 2. Brain parcellation mapped to a sample TBI subject.

shows the result of parcellation of WM surface of one subject with severe TBI. Parcellation is used to calculate lobe-specific surface-based (Sec. 2.2) and voxel-based biomarkers (Sec. 2.3).

Algorithm 2 Parcellation of biomarker of MRI with TBI

Input: Segmentation labels L, T1 MR image I, and the biomarker B at time point i, skull-stripped template of healthy brain H and associated brain parcellation label volume P_H.

Output: Parcellation label P_B for biomarker B at time point i.

1: Combine subject WM, GM, and CSF $\rightarrow M$
2: Use M to mask I to get skull-stripped image I_M.
3: Do affine registration from H to $I_M \rightarrow T_{H,i}$.
4: Apply the affine transformation $T_{H,i}$ to $P_H \rightarrow P$.
for (i, j, k) = each location of B with value but no parcellation label assigned **do**
  5: Search the nearest location with assigned parcellation label, assign the label value to $P_B(i, j, k)$.
**end for**

---

3. RESULTS

We apply our analysis to multimodal image data of five TBI patients with large lesions. Each subject was scanned at two time points, an acute scan at ≈ 5 days and another chronic scan at ≈ 6 months post injury. The image data of each subject include T1, T2, FLAIR, and GRE modalities. Fig. 3 illustrates T1 images of five subjects at the acute stage. We have access to three clinical scores per subject: Glasgow Coma Scale (GCS) at admittance, Glasgow Outcome Scale (GOS) at acute, and GOS at the chronic phase, scores which are routinely used in the literature [1, 2, 3, 4] for correlation with imaging findings.

We construct spatiotemporal models for each subject to obtain segmentations and deformation maps between acute and chronic time points [7], followed by calculation of the imaging biomarkers such as cortical thickness, volume, and deformation at every location in the brain. Fig. 4 (a) illustrates visualization of both cortical thickness and spatial displacement on the white matter surface at the acute time point, in which cortical thickness change is represented as scalar overlay and displacements are shown as arrows. Fig. 4 (b) shows the distributions of cortical thickness at acute and chronic time points for the whole brain, where a trend of cortical thickness decrease is observed.

Spearman's rank correlation was used to assess the monotonic dependence between imaging biomarkers and clinical scores. Our first analysis of biomarkers is about global correlation in which we analyze the relationship between whole-brain image findings and clinical scores. Table. 1 lists the
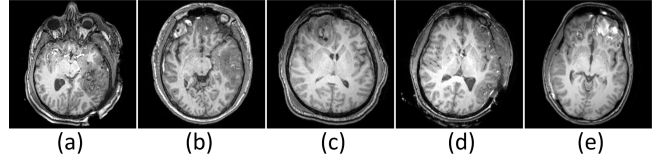
Fig. 3. Axial views of acute T1 images of five subjects, showing injury at different locations.
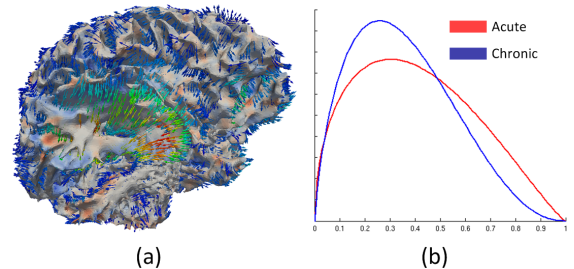
Fig. 4. Surface-based biomarkers shown for one subject: (a) Visualization of cortical thickness change and spatial displacement, (b) cortical thickness distributions at acute and chronic time points.

	GCS	GOS_1	GOS_2	Δ GOS
Cort. thick.	-0.0513	0.0000	-0.1581	-0.5270
Displ.	-0.4104	-0.7071	-0.3162	0.0000
WM volume	0.0513	0.7071	0.6325	0.7906
GM volume	0.3591	0.7071	-0.1581	-0.9487
CSF volume	-0.1026	-0.3536	-0.1581	-0.5270
NHL volume	-0.6669	0.0000	0.9487	0.9487
HL volume	0.0513	0.7071	0.9487	0.7379
Jac.	0.6669	0.7071	0.6325	0.3689

Table 1. Whole-brain correlations between imaging biomarkers and clinical scores. First row shows clinical scores, GOS_1 is the GOS at acute time point, GOS_2 is the GOS at chronic time point, Δ GOS = $GOS_2 - GOS_1$. The first column indicates image-derived features: cort. thick. is the cortical thickness, displ. is the mean of the spatial displacements. NHL denotes non-hemorrhagic lesion and HL denotes hemorrhagic lesion. Jac. is the mean of the log Jacobian determinant of the deformation field.

Spearman's correlation values between image-derived features and clinical scores, where imaging biomarkers (3D) at individual time points were used for correlation with GCS, GOS_1, and GOS_2 and changes of imaging biomarkers (4D) between time points were correlated with the differential Δ GOS score. In general, the top three correlated features are the Jacobian determinant of deformation field, volume of non-hemorrhagic lesion and volume of hemorrhagic lesion. We also find that the volume of non-hemorrhagic lesion has high correlation with acute GCS but no correlation with acute

GOS. Contrary to this, the volume of the hemorrhagic lesion has nearly no correlation with acute GCS but high correlation with acute GOS. Although preliminary on our small sample size, these observations may be of interest because both clinical scores are measurements for acute time point but show distinctive correlations with the two lesion types.

Regional analysis was conducted using brain parcellation for studying each major lobe separately, yielding information on the time trajectory of tissue after trauma. Fig. 5 shows the lobar correlation analysis, where we show the result on 14 major lobes. In general, the lobar analysis agrees with whole brain analysis but provides better insight on how different functional regions are related to clinical outcome. We find the correlations between GOS difference and the change of WM volume are complementary to the correlations between GOS difference and the change of GM volume. This finding agrees with the trend in whole-brain analysis showing GM volume decrease and WM volume increase in chronic MR scans.

4. CONCLUSIONS

We propose a new framework for computing imaging biomarkers by extending our recently developed spatiotemporal model construction. This generates full spatiotemporal information of imaging-related changes and provides descriptive visualizations of TBI-related structural changes. Preliminary results show that the top three correlated biomakers are Jacobian determinant of deformation field, volume of non-hemorrhagic lesion and of hemorrhagic lesion. Due to the small data set in this study, we do not draw any general conclusion from our analysis. However, we see our contribution as a first step to extract quantitative parameters from longitudinal multimodal imaging that will inform clinicians about brain and lesion changes due to impact, but also changes during recovery in regions not primarily affected by impact. In the future, we will evaluate the proposed methodologies using a larger data set, and also explore the addition of other modalities such as DTI, where a spatiotemporal model of connectomic changes would provide additional highly valuable information.

5. REFERENCES

[1] T.A.G.M. Huisman, L.H. Schwamm, P.W. Schaefer, W.J. Koroshetz, N. Shetty-Alva, Y. Ozsunar, O. Wu, and A.G. Sorensen, "Diffusion tensor imaging as potential biomarker of white matter injury in diffuse axonal injury," *AJNR*, vol. 25, no. 3, pp. 370–376, 2004.

[2] EA Wilde, SR McCauley, JV Hunter, ED Bigler, Z. Chu, ZJ Wang, GR Hanten, M. Troyanskaya, R. Yallampalli, X. Li, et al., "Diffusion tensor imaging of acute mild traumatic brain injury in adolescents," *Neurology*, vol. 70, no. 12, pp. 948–955, 2008.
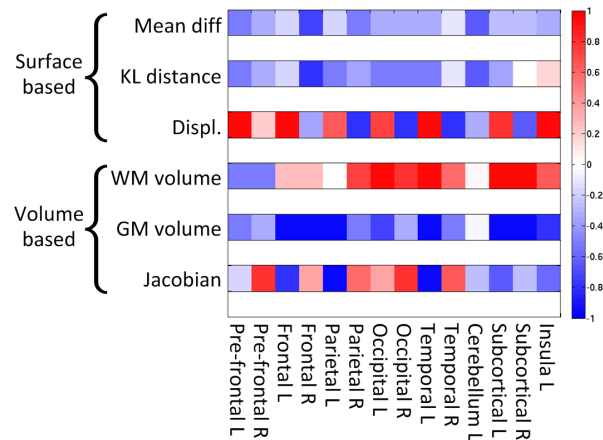
Fig. 5. Lobar correlation analysis between the change of imaging biomarkers (4D) and the change of clinical scores. Rows indicate imaging biomarkers, from top to bottom: difference of mean value of cortical thickness (chronic minus acute), KL distance between two distributions of cortical thickness, mean of spatial displacement, difference of volume of WM, difference of volume of GM, and mean of log Jacobian determinant of deformation field. Columns indicate different lobes.

[3] A. Sidaros, A.W. Engberg, K. Sidaros, M.G. Liptrot, M. Herning, P. Petersen, O.B. Paulson, T.L. Jernigan, and E. Rostrup, "Diffusion tensor imaging during recovery from severe traumatic brain injury and relation to clinical outcome: a longitudinal study," *Brain*, vol. 131, no. 2, pp. 559–572, 2008.

[4] J.M. Ling, A. Peña, R.A. Yeo, F.L. Merideth, S. Klimaj, C. Gasparovic, and A.R. Mayer, "Biomarkers of increased diffusion anisotropy in semi-acute mild traumatic brain injury: a longitudinal perspective," *Brain*, vol. 135, no. 4, pp. 1281–1292, 2012.

[5] J. Kim, B. Avants, S. Patel, J. Whyte, B.H. Coslett, J. Pluta, J.A. Detre, and J.C. Gee, "Structural consequences of diffuse traumatic brain injury: a large deformation tensor-based morphometry study," *Neuroimage*, vol. 39, no. 3, pp. 1014–1026, 2008.

[6] A. Irimia, B. Wang, S.R. Aylward, M.W. Prastawa, D.F. Pace, G. Gerig, D.A. Hovda, R. Kikinis, P.M. Vespa, and J.D. Van Horn, "Neuroimaging of structural pathology and connectomics in traumatic brain injury: Toward personalized outcome prediction," *NeuroImage: Clinical*, vol. 1, no. 1, pp. 1–17, 2012.

[7] B. Wang, M. Prastawa, S.P. Awate, A. Irimia, M.C. Chambers, P.M. Vespa, J.D. van Horn, and G. Gerig, "Segmentation of serial mri of tbi patients using personalized atlas construction and topological change estimation," in *IEEE ISBI*, 2012, pp. 1152–1155.